ICAS-84-1.7.3 FLUTTER CALCULATION ON A SUPERCRITICAL WING IN THE TRANSONIC RANGE COMPARISON THEORY-EXPERIMENT

A. Gravelle, ONERA, Chatillon, France,
H. Hönlinger, MBB-Munich, FRG,
S. Vogel, MBB-Bremen, FRG

## Abstract

Supercritical wings are characterized by a high sensitivity of the flutter speed to the parameters like incidence or Mach number. On the other hand, the classical linear method (doublet lattice) is shown to be often inadequate. This study was undertaken with two wind tunnel models:

- one of them is a "rigid" model used for steady and unsteady pressure measurements.
- the other one is a flexible model with which it is possible to achieve transonic flutter speeds.

The flutter model was equipped with a flutter suppressor device, which gave the possibility of exploring the domain in which the model was naturally unstable. The model could be excited in order to make possible the determination of the poles of the transfer functions in open or closed loops.

A series of flutter calculations using experimental corrections, which took into account the results of the various test cases, was undertaken.

## Table of contents



## I. Introduction

A few years ago, some studies were undertaken in different countries to demonstrate the variation of critical flutter speed versus incidence for given Mach numbers. This phenomenon is particularly sensitive for an aircraft equipped with supercritical wings, (1), (2).

Up to now few calculations were able to take into account the non-linear effect due to incidence and the resulting untwist of the wing in unsteady flow. This study shows a tentative comparison between calculation and tests using two different theoretical approaches.

The first theory starts with wind tunnel measurements of steady pressure made on a "rigid" model for different incidences. A spanwise correction by means of steady measured pressures is applied, allowing to linearize the problem around each section incidence. One advantage of this method is to take into account, with the help of the applied correction, the steady viscous effect due to the boundary layer. The disadvantage is that the correction is not able to take correctly into account the interaction between the different strips.

The second method is a three-dimensional computation based on the transonic small perturbation (TSP) equation taking into account the real deformation of the profile under a given steady load. (For this computation the deformation was calculated starting from the measurement of the load distribution). This method in its present application does not take into account the viscous effect.

An extensive wind tunnel test program on this subject was performed in the ONERA S2 transonic pressurized wind tunnel to generate a basis for the comparison. Sensitive differences appeared on the critical dynamic pressure as well as on the violence of the flutter.

## II. Choice of the model

### II.1 Description of the flutter model selected for the test

To substantiate the two new theoretical studies by wind tunnel tests, a flutter model had to be designed taking into account all constraints deriving from the wind tunnel, the model suspension system and fabrication requirements. It was decided to use a half wing model with dummy fuselage. The model wing geometry, its supercritical profile, external shape of the engine as well as the stiffness and mass properties of the wing was similar to a modern transport aircraft.

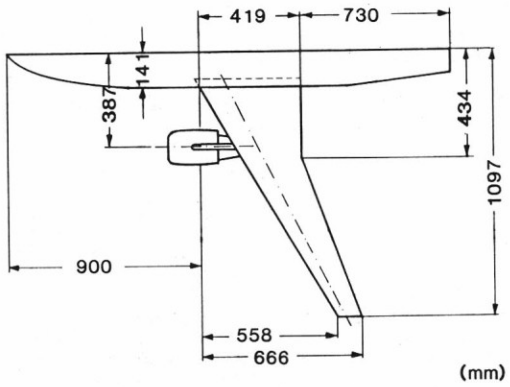


FIG. 1 MODEL GEOMETRY

Fig. 1 shows the dimensions of the half wing model. The model installation on the tunnel wall in the ONERA transonic pressurized wind tunnel can be seen in Fig. 2.

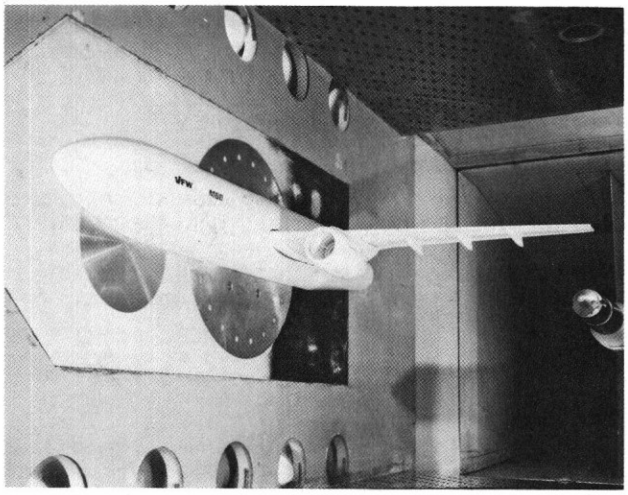

FIG. 2 MODEL MOUNTED ON THE TUNNEL WALL ( ONERA S2-MA )

To use this flutter model successfully for the rather sophisticated wind tunnel test program a flutter model like this must have the following new features. The supercritical profile of the wing model has to be manufactured with high pecision. The jig shape of the wing model has to be well defined to get a distinct difference to the flight shape during wind tunnel test. A precise variation of the angle of attack without changing any elastic properties of the wing model and the suspension system has to be achieved.

In addition to these mainly geometrical requirements the model must be able to reproduce clearly the expected changes in the flutter speed. These changes were supposed to be caused by non-linearities like twist induced angle of attack and Mach number effects. In order to avoid measurement problems and especially to explore small changes in flutter speed the model must have violent flutter characteristics, well within the tunnel range.

It is difficult to fulfil this dynamic requirement with a flutter model design similar to a real aircraft. Because a real aircraft design must be flutter free within its flight envelope the flutter speed of the similar model will be very high too. To create the needed violent flutter case, it was decided to modify only engine mass data and wing root conditions. The wing stiffness and mass properties as well as the engine attachment stiffness should be kept similar to a real aircraft design. By this measure the typical flutter mechanism of a modern transport aircraft should not be changed significantly.

II.2 Determination of a violent flutter case

During the design phase of the model a parametrical study was performed to create the needed violent flutter case well within the pressure range of the ONERA S2 wind tunnel. In this study a simple mathematical model including the root condition was used. The wing stiffnesses were represented by a torsion box. The wing masses and inertia were simulated by lumped masses. For the engine attachment measured influence coefficients of the real model pylon were introduced. The half-wing root conditions were simulated by a cruciform beam. This special element allows the variation of the torsion and bending stiffness independently of each other within a certain band width.

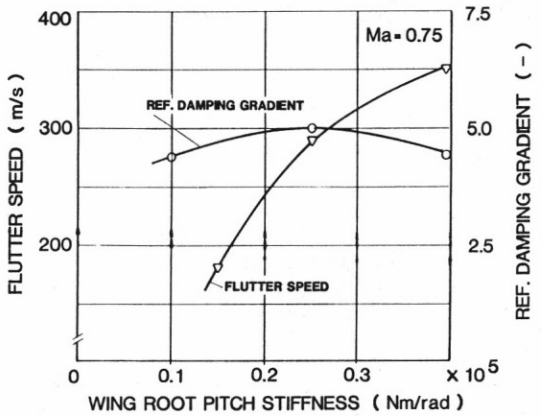


FIG. 3 MODEL FLUTTER SPEED VS WING ROOT PITCH STIFFNESS

Extensive flutter trend studies were performed with the mathematical model by varying engine mass data and wing root stiffness conditions within reasonable ranges. The results of this exercise are summarized in Figs. 3 and 4. As can be seen from Fig. 3 the flutter speed is highly dependent on wing root torsion stiffness, whereas the damping gradient of the flutter model stays nearly unchanged. Fig. 4 however shows that the damping gradient of the flutter model can be considerably increased by reducing the engine mass. But this includes also an increase of the flutter speed. It was also found that the wing-root bending attachment stiffness should be as high as possible in order to shift the

nodal line of the flutter-sensitive mode rearward as much as possible. This was recognized to be the major cause of flutter.

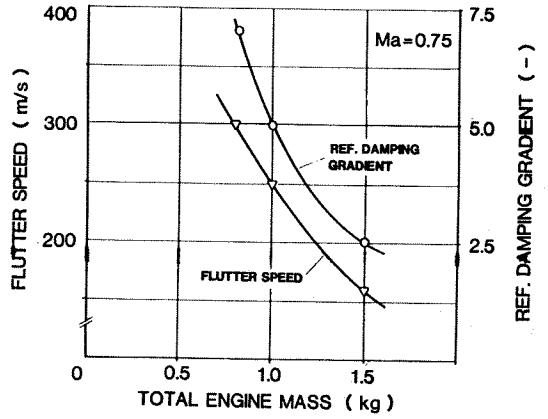


FIG. 4 MODEL FLUTTER SPEED VS ENGINE MASS

Combining these theoretical results a violent flutter case can be created when the model design is modified as follows:

The engine mass of the nominal design (similar to the real aircraft design) has to be decreased by 30%. To meet the flutter critical wing root conditions a cruciform section beam suspension with very low torsional stiffness has to be designed. To achieve the required very high bending attachment stiffnesses a rotable roller bearing has to be implemented at the wing root clamping point to support the cruciform beam (cross spring).

## III. Realisation

### III.1 Wing mount with actuator and equipment

In the wind tunnel the cross spring supporting the model was bolted to a large plate attached to the turntable at the wind tunnel wall. An oscillating hydraulic actuator fixed on the same plate was capable to create pitch motion of the wing, the torque being transmitted through a small shaft located inside the cruciform beam. Fig. 5.

1 WING MODEL
2 ROOT STIFFNESS CONDITIONS
3 TRANSMITTER AXIS
4 INFINITE CLAMPING
5 FLECTOR SYSTEM
6 ACTUATOR

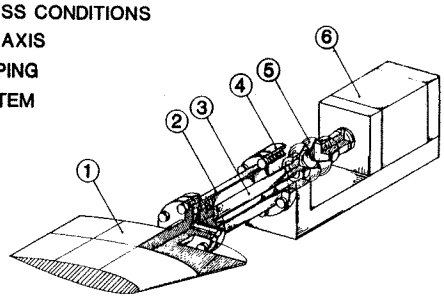


FIG. 5 MODEL EXCITATION THROUGH SUSPENSION

The additional stiffnesses in bending and torsion due to the actuator were negligible due to the dimension of the transmission shaft and the presence of a flector eliminating radial strains, Fig. 6.

The model was equipped with 10 accelerometers (6 in the wing, 4 in the engine), 2 strain gauge bridges for bending and torsion bonded on the cross spring. The actuator position was controlled by means of a potentiometer.

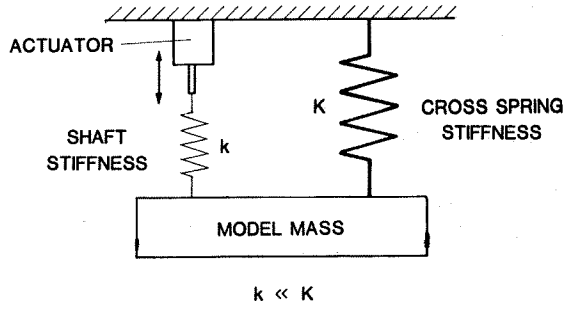


FIG. 6 IDEALIZED MODEL EXCITATION SYSTEM

### III.2 Eigenmodes (GVT)

The eigenmodes were measured with the model being mounted in the wind tunnel. The modes having the largest influence on flutter were: wing bending mode of 36 Hz, engine yaw mode at 46 Hz (very similar to the bending mode on the wing), and the engine pitch mode at 56 Hz, inducing a pitch motion of the wing. The fourth mode, at 67 Hz was measured but had little influence on the flutter in this case.

### III.3 Preliminary flutter calculation using linear theory (Doublets)

The preliminary flutter computations were done starting from the mode shapes, generalized masses and stiffnesses measured in laboratory. A doublet lattice method was used which does not take into account the incidence of the model. 152 doublets were distributed on the wing.

Unsteady aerodynamic forces were also computed on the engine considered as a circular wing using the doublet lattice theory (3). To illustrate the importance of nacelle airloads, one should note that the part due to the engine in the diagonal term of the generalized aerodynamic force of the pitch motion presents 32% of the total force. The structural damping was not included in this calculation.

Fig. 7 shows calculated violent flutter for the basic configuration at Mach number 0.78, the critical stagnation pressure being about 1.1 bars. This result is in good agreement with the study requirements, giving a comfortable margin in the wind tunnel stagnation pressure range (from 0.2 to about 1.6 bars at such Mach number).

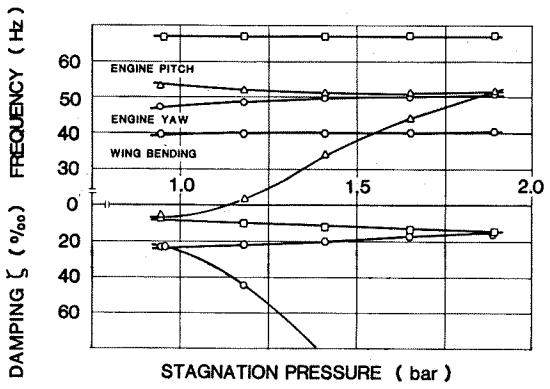


FIG. 7 LINEAR FLUTTER CALC. - BASIC CONFIGURATION

III.4 Active flutter suppression

An active flutter suppression system was applied, using, as input, the torque of the root section of the wing, measured by the strain gauge bridge on the cross spring. This signal was fed back to the actuator through a combination of band-pass and notch filters in order not to influence the modes which are not involved in the flutter phenomenon (Fig. 8). Then through the soft shaft it creates a pitch moment at the root of the wing which is mainly a damping moment for the engine pitch mode (90 degrees phase lead). The increase of damping due to the feedback system without wind is given in Fig. 9, as a function of the gain of the loop.

The linear computation for the controlled model by means of the doublet lattice theory (Fig. 10) shows the efficiency of this system in the whole stagnation pressure range at Mach number 0.78.

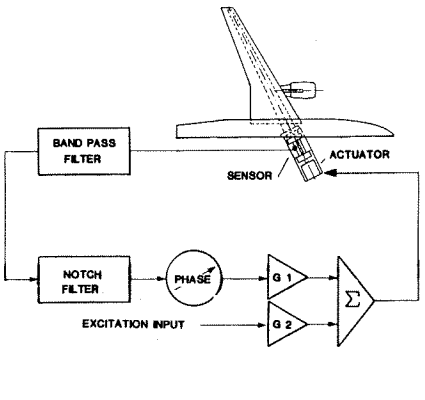


FIG. 8 BLOCKDIAGRAM OF THE CONTROL SYSTEM

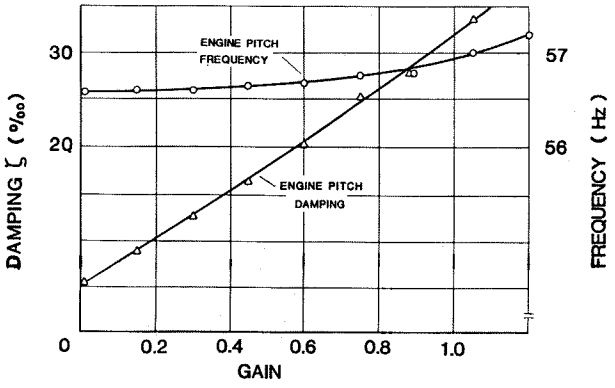


FIG. 9 DAMPING AND FREQUENCY VS FLUTTER SUPPRESSOR GAIN

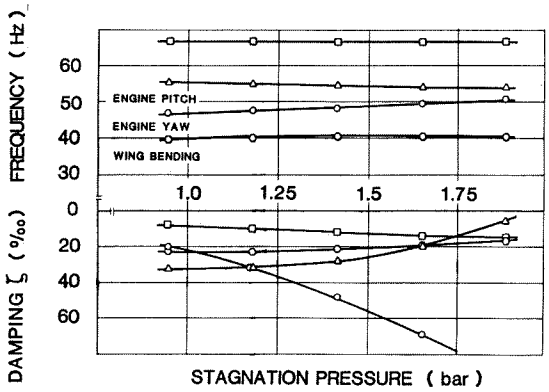


FIG. 10 LINEAR FLUTTER CALC. WITH FLUTTER SUPPRESSION

Though the engine yaw mode has a lower damping, the pitch mode is damped and the frequencies are well separated due to the modification of the coupling terms, and due to a stiffness effect induced by the unsteady aerodynamic forces created by the pitching moment of the wing. (The pitch mode frequency is higher). This control allowed to perform measurements at stagnation pressures higher than the critical stagnation pressure, and therefore to deduce negative damping in some of the cases.

## IV. Wind tunnel results

IV.1 Incidence and Mach number influence

Figure 11 shows a strong incidence effect, at Mach number 0.78, on the damping of the engine pitch mode. Increasing the incidence, i.e. in-

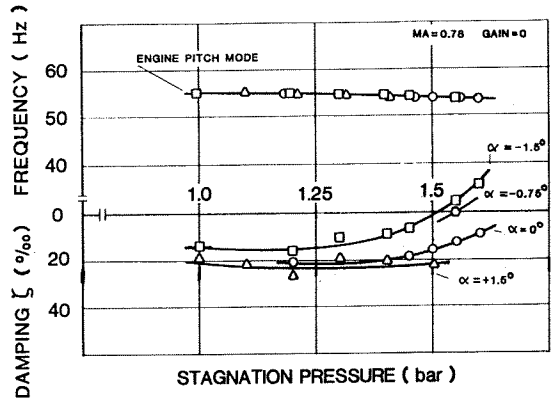


FIG. 11 VARIATION OF FLUTTER SPEED DUE TO INCIDENCE

creasing the steady aerodynamic loads, increases the damping whereas the frequency of the same mode is not affected.

On Figure 12 one can see that a variation of the Mach number between 0.78 and 0.82 has no effect on both the frequency and the damping of the flutter mode.

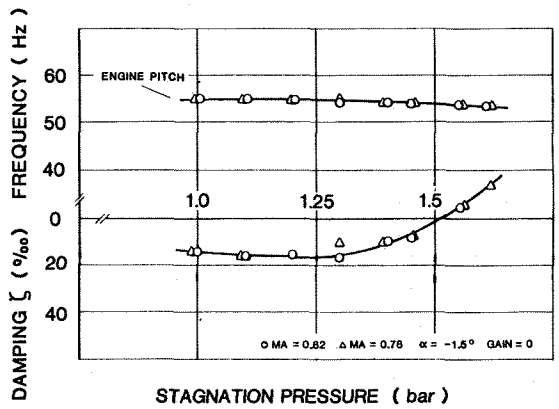


FIG. 12 MEASURED MACH NUMBER EFFECT ON ENGINE PITCH MODE

IV.2 Flutter suppression system influence

Figure 13 shows the effect of the flutter suppression system at Mach number 0.78 and -1.5° incidence. As predicted by the calculation the pitch mode frequency is slightly higher, the pitch mode has a positive damping which decreases beyond the non-controlled-system flutter stagnation pressure. The effect of the control on the engine yaw mode is more pronounced as predicted, where the damping reaches quite low values, though the calculation shows already the tendency to lower damping.

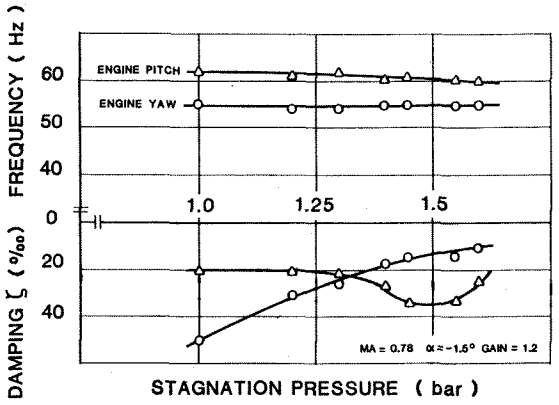


FIG. 13 EFFECT OF THE CONTROL SYSTEM ( MEASURED )

## V. Interpretation

V.1 Linear calculation using steady correction

In the transonic region the unsteady airforces and therefore the flutter behaviour depend on the steady airloads, and therefore also on the elastic deformation of the wing. The steady airforces for a given wing are determined by Mach number and spanwise incidence distribution. One model was used in wind tunnel tests for measurements of loads and pressure distributions. This pressure model has a given characteristic spanwise incidence distribution corresponding to the aircraft flight shape under normal cruising condition. The model is considered to be stiff enough so that the incidence distribution is not significantly changed by variation of dynamic pressure.

The elastic deformation of the flexible flutter model under steady airload was estimated by the Rayleigh-Ritz method using measured mode shapes and generalized masses and stiffnesses. Fig. 14 shows the spanwise twist distribution for different stagnation pressures for 1.5° incidence, and Fig. 15 for -1.5°incidence.

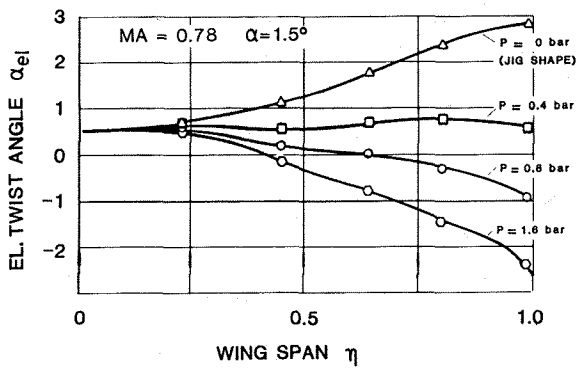


FIG. 14 STREAMWISE ELASTIC TWIST ANGLE VS SPAN

Using the assumption that spanwise strips can be treated separately (2-D flow), the steady lift and pitch moment coefficients were estimated for various incidence distribution by analyzing the test results of a WT model for static pressure measurements which corresponds to the airplane flight shape.

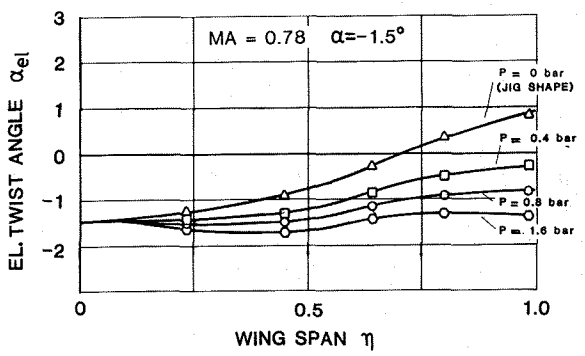


FIG. 15 STREAMWISE ELASTIC TWIST ANGLE VS SPAN

Fig. 16 shows the spanwise lift and pitch moment coefficients for $\alpha$ = 1.5°, and Fig. 17 for the case with $\alpha$ = -1.5°. There is obviously a strong change in lift distribution, but nearly

no change in pitch moment due to the strong rear loading of the supercritical wing.

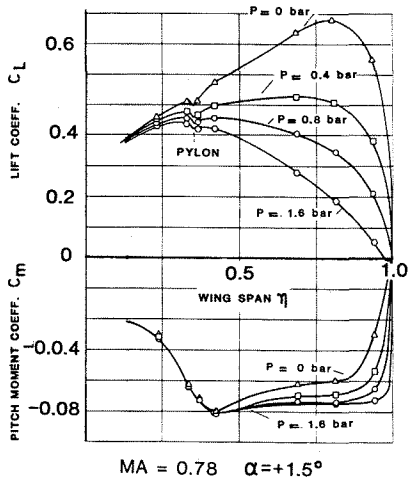


FIG. 16 LIFT AND PITCH MOMENT COEFF. VS SPAN

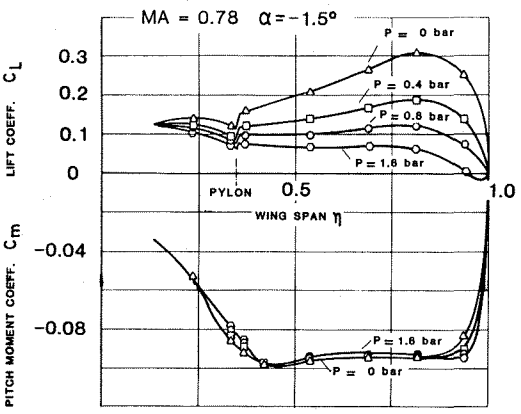


FIG. 17 LIFT AND PITCH MOMENT COEFF. VS SPAN

For calculating the unsteady airloads in the transonic region the theoretical values have to be corrected for elastic deformation to give at least the right tendency in this critical regime. The more elaborate theoretical 3D transonic methods for the calculation of unsteady airloads in the transonic regime for different steady-state conditions are at present too expensive to be applied routinely by a manufacturer. Therefore, a simple correction based on spanwise lift curve slope $C_{L\alpha}$ and local aerodynamic centre location $X_{ac}$ was used for the correction of the generalized airforces calculated by Laschka's method using measured mode shapes of the model. This method includes the two following assumptions:

1. the correction is derived for the pitching motion, but is also applied to plunging motion,

2. the quasisteady corrections are applied in the full frequency range.

Apart from the fact that here a 3D theoretical subsonic method is used, the basis is similar to the "Modified strip analysis" of E.C. Yates, Jr. that is extended here also to the transonic region (4). The variation of measured $C_{L\alpha}$ and $X_{ac}$ with $\alpha$ for some outer wing sections, for two transonic Mach numbers is shown in Fig. 18. This figure shows the non-linear behaviour of the outer wing lift curve slope with incidence especially for Mach = 0.78, with a minimum value at $\alpha \approx 0$, whereas the aerodynamic centre moves backward with decreasing incidence, until a value where it suddenly shifts forward.

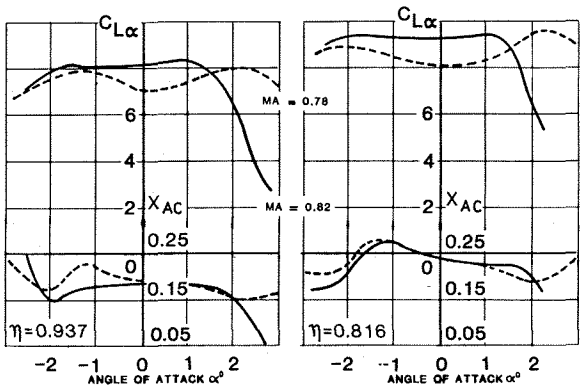


FIG. 18 SECTIONAL LIFT CURVE SLOPE $C_{L\alpha}$ AND AERODYN. CENTER LOCATION $X_{AC}$ VS ANGLE OF ATTACK

Using the estimated spanwise incidence distribution for the possible wind tunnel stagnation pressures for given Mach numbers, correction terms were formed to account for the sectional lift curve slope and aerodynamic centre location, and unsteady airforces were calculated with these corrections for performing flutter calculations.

The additional input data for the flutter calculation were the measured generalized masses and eigenfrequencies including the structural damping of the modes.

The effect of static aeroelastic deformation on frequency and damping behaviour is shown in

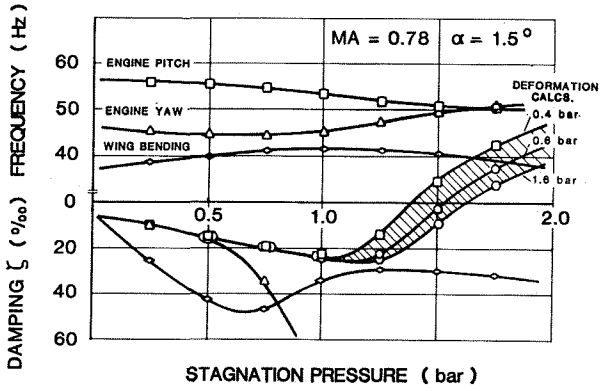


FIG. 19 INFLUENCE OF ELASTIC WING DEFORMATION ON THE FLUTTER BEHAVIOUR

the Fig. 19 for some investigated stagnation pressures. From this figure it is visible that for the investigated wing the flutter speed increases with increasing static aeroelastic deformation, whereas in the case with low static airload (for $\alpha$= -1.5°) the influence of increasing pressure is small.

V.2 Transonic small perturbation calculation

The method is a true three-dimensional transonic small perturbation method (5), to calculate steady airloads as well as unsteady ones. It uses an alternating direction implicit procedure which was proposed by Ballhaus (6).This method in its present form models the airfoil shape and local incidence, but not the viscous effects.
Computations were done in two different cases: the first one uses the "jig shape" of the model, i.e. the shape of the model without load, the second one uses the model shape under airloads corresponding to one of the wind-tunnel conditions (M=0.78; Pi = 1.4 bars). The deformation of the model under airload was measured in laboratory by simulating these loads with distributed masses. The load distribution on the wing was known from previous measurements using a rigid model with the same geometry. The difference in the twist at the tip of the wing reaches about 2 degrees in this case.

Fig. 20 shows the steady lift coefficient $C_L$ as function of the span of the wing. The difference between the two cases is very important near the tip of the wing, where the twist angle variation is the most important and lower at the root of the wing where the twist angle difference is only 0.4° due to the flexibility of the cross spring.

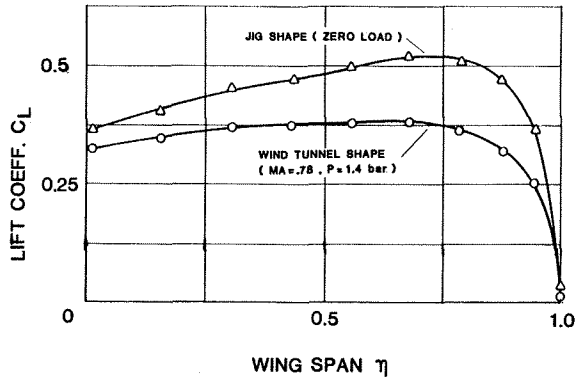


FIG. 20 STEADY LIFT DISTRIBUTION VS WING SPAN

Fig. 21 shows the quasi-steady spanwise lift and moment derivatives for a pitch motion. These coefficients are not so sensitive to the twist variation, except the moment coefficient in the vicinity of the wing tip. The unsteady results of this calculation are not yet available, but from the quasi-steady results shown in Fig. 21, one can assume that the damping and frequency curve patterns will not be very different. The effect of the twist under load is to decrease both lift and pitch moment derivatives, so that we can expect a critical flutter stagnation pressure slightly higher in this case, as it was observed by the first calculation method as well as during the wind-tunnel tests.

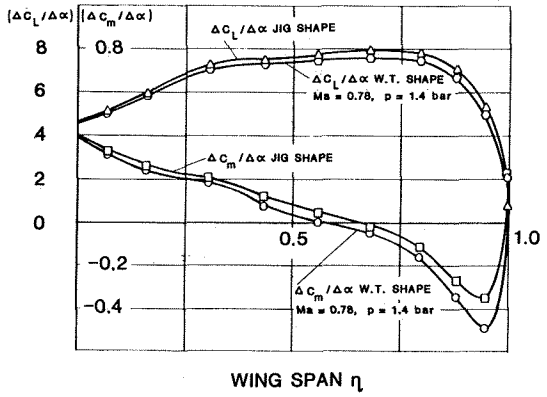


FIG. 21 QUASI-STEADY LIFT AND MOMENT COEFF.- TSP THEORY

## VI. Conclusion

Wind tunnel flutter tests on a supercritical transport aircraft type wing, at transonic Mach numbers, showed a large influence of small variations of the angle of attack. These tests were achieved by using a new kind of wing mount allowing to apply pitch excitation as well as active flutter control on the wing by means of a hydraulic actuator, facilitating an accurate determination of the flutter condition. Different calculation methods taking into account thickness, incidence and resulting untwist of the wing were applied.
The first one uses corrections based on quasi-steady test results for the estimated load-dependent incidence applied to Laschka's linear subsonic method. A comparison of the thus calculated and the measured frequency and damping behaviour versus stagnation pressure for M = 0.78 and $\alpha$= 0° is shown in Fig. 22. The calculated values show also the influence of unsteady aerodynamic forces on the nacelle, changing the flutter point from non-conservative to conservative.

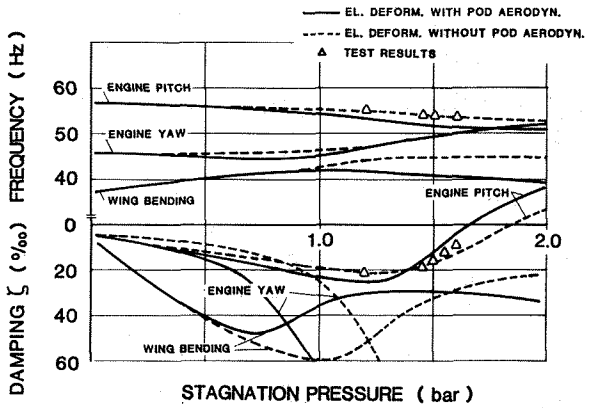


FIG. 22 COMPARISON OF CALCULATIONS AND TEST RESULTS
MA = 0.78 $\alpha$ = 0°

The second method is a fully theoretical three-dimensional transonic small perturbation method.

In both cases, the same trend was observed: the aeroelastic deformation of the wing under steady airload (at positive incidences) leads to an increase in the critical flutter stagnation pressure, whereas the increasing stagnation pressure itself has no influence on the flutter behaviour as shown for low steady load conditions. This tendency could be observed in an even more pronounced manner in wind-tunnel tests.

## VII. References


(1) E. Carson Yates, Jr., Eleanor C. Wynne and Moses G. Farmer
Effects of angle attack on transonic flutter of a supercritical wing
Journal of Aircraft, Vol. 20, No. 10, October 1983

(2) A.J. Persoon, J.J. Horsten and J.J. Meijer On measuring transonic dips in the flutter boundaries of a supercritical wing in the wind tunnel
AIAA-83-1031-CP, May 1983

(3) J.J. Angélini, S. Chopin, R. Destuynder
Forces aérodynamiques instationnaires induites par les vibrations aéroélastiques d'un réacteur en nacelle
La Recherche Aérospatiale no 1974-4

(4) E.C. Yates Jr., E.C. Wynne, M.G. Farmer and R.N. Desmarais
Prediction of transonic flutter for a supercritical wing by modified strip analysis and comparison with experiment
AIAA-Paper 81-0609, 1981

(5) P. Mulak, M. Couston, J.J. Angélini
Extension of the transonic perturbation approach to three-dimensional problems
International Symposium on Aeroelasticity
Nuremberg, October 5-7, 1982

(6) W.F. Ballhaus, P.M. Goorjian
Implicit finite difference computations of unsteady transonic flows about airfoils AIAA paper 77-205, January 1977